ARTICLE NO. 79-4110

Dynamic Response of Axisymmetric Solids Subjected to Impact and Spin

Gordon R. Johnson*
Honeywell, Inc., Hopkins, Minn.

A numerical method is presented to obtain solutions for axisymmetric solids subjected to impact and spin. The method is based on a finite element formulation wherein the equations of motion are integrated directly rather than through the traditional stiffness matrix approach. The formulation is given for axisymmetric triangular elements which can experience large strains and displacements in the radial, axial, and angular directions. The effects of material strength and compressibility are included to account for elastic-plastic flow and wave propagation. The addition of angular displacements allows the effect of twisting to be included in the analysis. The radial and axial equations of motion are applied in the usual manner, whereas the angular (spin) equations of motion are obtained by conserving angular momentum; this allows the angular velocities of the nodes to be altered by a change in radial position and/or shear stress induced tangential forces acting on the concentrated masses. The numerical method can also be used to obtain steady-state solutions for spinning solids.

Introduction

A COMMON loading condition for axisymmetric solids is the combination of spin and impact. Although there are many two-dimensional computer codes available to compute the response due to impact,[1-4] the effect of spin is usually ignored. This paper presents a numerical method that allows the spinning effect to be included. It is an extension of the formulation in the EPIC code,[1] which is based on a finite element Lagrangian technique, where the equations of motion are integrated directly rather than through the traditional stiffness matrix approach. In addition to the inclusion of spin, the present formulation is valid for the general class of dynamic responses, whereas the original EPIC code was primarily intended only for high-velocity impact problems. The high-velocity limitation was imposed since the material was treated as rigid-plastic after the onset of yielding. As a result, elastic effects were ignored thereafter. The present EPIC-2 code computes stresses on an incremental basis such that both elastic and plastic stresses are considered at all times. This allows for elastic "snapback" which can be important for lower velocity impact. An additional feature of the computational technique is the ability to obtain steady-state solutions for spinning bodies.

Formulation

A schematic representation of the computational technique is shown in Fig. 1. The first step in the process is to represent the geometry with triangular elements having specific material characteristics. For the work presented herein, triangular elements are used, since they are well suited to represent the severe distortions that often occur during high-velocity impact.[1] Then the distributed mass is lumped at the nodes (element corners), and initial velocities are assigned to represent the motion at impact.

After the initial conditions are established, the integration loop begins as shown in Fig. 1. The first step is to obtain displacements and velocities of the nodes. If it is assumed the lines connecting the nodes (element edges) remain straight, then the displacements and velocities within the elements must vary linearly. From these displacements and velocities, the strains and strain rates within the elements can be obtained. Since the strains and strain rates are generally derivatives of linear displacement and velocity functions within the elements, the resulting strains and strain rates are generally constant within the elements.

The stresses in the elements are determined from the strains, strain rates, internal energies, and material properties. The stresses are obtained by combining elastic or plastic deviator stresses with hydrostatic pressure. The deviator stresses represent the shear-strength capability of the material, and the hydrostatic pressure is obtained from the volumetric strain and internal energy of the element. An artificial viscosity is also included to damp out localized oscillations caused by representing continuous media with lumped masses.

After the element stresses are determined, it is necessary to obtain concentrated forces at the nodes. These forces are statically equivalent to the distributed stresses within the elements and are dependent on the element geometry and the magnitude of the stresses. When the concentrated forces are applied to the concentrated masses, the nodal accelerations are defined, and the equations of motion are applied to determine new displacements and velocities. The integration loop is then repeated until the time of interest has elapsed.

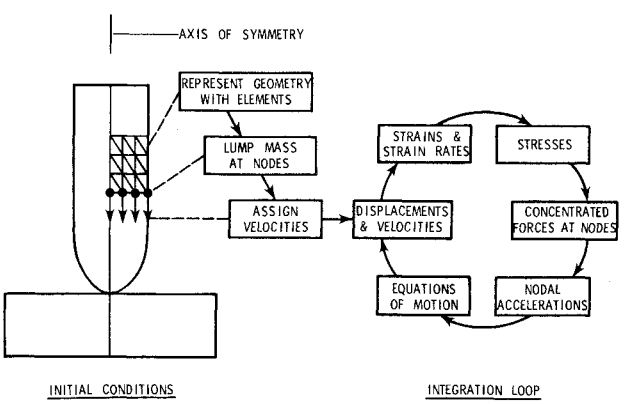

Fig. 1 Schematic representation of the finite element computational technique.

Received April 10, 1978; revision received Nov. 2, 1978.

Index categories: Aeroelasticity and Hydroelasticity; Computational Methods; Structural Dynamics.

*Engineering Fellow, Defense Systems Division.

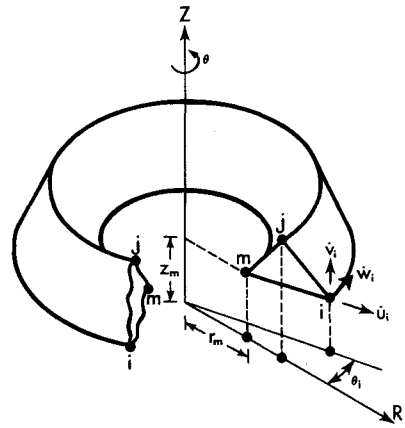

Fig. 2 Geometry of an axisymmetric element.

Geometry

A typical axisymmetric triangular element is shown in Fig. 2. It is geometrically defined by nodes *i, j,* and *m*, with the mass of the element being equally distributed to concentrated masses at the nodes. When a node is contained by more than one element, the total mass at node *i*, $\bar{M}_i$, is equal to one-third the mass of all elements that contain that node. For an axisymmetric finite element model, the concentrated masses can be visualized as concentric circular rings contained in planes that are perpendicular to the axis of revolution. These rings can move up and down along the axial direction (*Z* axis) and can expand and contract in the radial direction (*R* axis). In addition, they are allowed to experience rotations θ about the axis of revolution. The coordinates of node *i* are designated r_i, z_i, θ_i, and the radial, axial and tangential velocities are designated $\dot{u}_i$, $\dot{v}_i$, $\dot{w}_i$, where $\dot{w}_i = r_i\dot{\theta}_i$.

Strains and Strain Rates

The incremental strains which occur during each cycle of integration are obtained by mutiplying the strain rates by the integration time increment. The strain rates are obtained from the current geometry of the element and the velocities of the nodes. If it is assumed that the lines connecting the nodes remain straight, then the displacements and velocities within each element must vary in a linear manner. Then the velocities within the element can be expressed as

$$\dot{u} = \alpha_1 + \alpha_2 r + \alpha_3 z \tag{1}$$

$$\dot{v} = \alpha_4 + \alpha_5 r + \alpha_6 z \tag{2}$$

$$\dot{w} = \alpha_7 + \alpha_8 r + \alpha_9 z \tag{3}$$

where $\alpha_1 \ldots \alpha_9$ are geometry and velocity-dependent constants. It is possible to solve for α_1, α_2, α_3 by substituting the radial velocities and coordinates of nodes *i, j, m* into Eq. (1). This gives three equations and three unknowns such that Eq. (1) can be expressed in terms of the element geometry and nodal velocities.

$$\dot{u} = \frac{1}{2A}\left[(a_i + b_i r + c_i z)\dot{u}_i + (a_j + b_j r + c_j z)\dot{u}_j + (a_m + b_m r + c_m z)\dot{u}_m\right] \tag{4}$$

where $a_i = r_j z_m - r_m z_j$, $b_i = z_j - z_m$, $c_i = r_m - r_j$, and A is the cross-sectional area of the element in the *R-Z* plane. The other velocities ($\dot{v}$, $\dot{w}$) are identical to Eq. (4) except that the radial velocities are replaced by the axial and tangential velocities.

After the velocities are obtained, it is possible to determine the normal strain rates ($\dot{\epsilon}_r$, $\dot{\epsilon}_z$, $\dot{\epsilon}_\theta$), the shear strain rates ($\dot{\gamma}_{rz}$, $\dot{\gamma}_{r\theta}$, $\dot{\gamma}_{z\theta}$), and the localized rotational spin rate of the element in the *R-Z* plane (ω_{rz}).

$$\dot{\epsilon}_r = \frac{\partial \dot{u}}{\partial r} \tag{5}$$

$$\dot{\epsilon}_z = \frac{\partial \dot{v}}{\partial z} \tag{6}$$

$$\dot{\epsilon}_\theta = \frac{\bar{\dot{u}}}{\bar{r}} \tag{7}$$

$$\dot{\gamma}_{rz} = \frac{\partial \dot{u}}{\partial z} + \frac{\partial \dot{v}}{\partial r} \tag{8}$$

$$\dot{\gamma}_{r\theta} = \frac{\partial \dot{w}}{\partial r} - \frac{\bar{\dot{w}}}{\bar{r}} \tag{9}$$

$$\dot{\gamma}_{z\theta} = \frac{\partial \dot{w}}{\partial z} \tag{10}$$

$$\omega_{rz} = \frac{1}{2}\left(\frac{\partial \dot{v}}{\partial r} - \frac{\partial \dot{u}}{\partial z}\right) \tag{11}$$

It can be seen that Eqs. (5), (6), (8), (10), and (11) are derivatives of linear functions and are therefore constant within the element. Equations (7) and (9) involve averages of the nodal velocities ($\bar{\dot{u}}$ and $\bar{\dot{w}}$) and the three radii ($\bar{r}$), so they are not necessarily constant. It is also necessary to use an equivalent strain rate which is expressed as

$$\bar{\dot{\epsilon}} = \Big[(2/9)[(\dot{\epsilon}_r - \dot{\epsilon}_z)^2 + (\dot{\epsilon}_r - \dot{\epsilon}_\theta)^2 + (\dot{\epsilon}_z - \dot{\epsilon}_\theta)^2 + (3/2)(\dot{\gamma}_{rz}^2 + \dot{\gamma}_{r\theta}^2 + \dot{\gamma}_{z\theta}^2)]\Big]^{1/2} \tag{12}$$

An equivalent plastic strain $\bar{\epsilon}_p$ gives a measure of the distortion in the element and can be used to determine strain hardening effects for the material stength. It is obtained by integrating $\bar{\dot{\epsilon}}$ with respect to time during plastic flow.

$$\bar{\epsilon}_p{}^{t+\Delta t} = \bar{\epsilon}_p{}^{t} + \bar{\dot{\epsilon}}\Delta t \tag{13}$$

where Δt is the integration time increment. It should also be noted that subsequent computations will involve deviator strain rates ($\dot{e}_r, \dot{e}_z, \dot{e}_\theta$) which are readily obtained from the normal strain rates ($\dot{\epsilon}_r, \dot{\epsilon}_z, \dot{\epsilon}_\theta$).

Stresses and Pressures

The stresses in the elements are determined from the strains, strain rates, internal energies, and material properties. The three normal stresses ($\sigma_r, \sigma_z, \sigma_\theta$) are expressed in terms of deviator stresses (s_r, s_z, s_θ), hydrostatic pressure P, and artifical viscosity Q.

$$\sigma_r = s_r - (P+Q) \tag{14}$$

$$\sigma_z = s_z - (P+Q) \tag{15}$$

$$\sigma_\theta = s_\theta - (P+Q) \tag{16}$$

Trial values of the deviator stresses at time $= t + \Delta t$ are

$$s_r^{t+\Delta t} = s_r^t + 2G\dot{e}_r\Delta t - 2\tau_{rz}^t\omega_{rz}\Delta t \tag{17}$$

$$s_z^{t+\Delta t} = s_z^t + 2G\dot{e}_z\Delta t + 2\tau_{rz}^t\omega_{rz}\Delta t \tag{18}$$

$$s_\theta^{t+\Delta t} = s_\theta^t + 2G\dot{e}_\theta\Delta t \tag{19}$$

In Eq. (17) the first term (s_r^t) is the radial stress at the previous time, and the second term ($2G\dot{e}_r\Delta t$) is the incremental stress due to the incremental strain ($\dot{e}_r\Delta t$) during that time increment, where G is the elastic shear modulus. The third term ($2\tau_{rz}^t\omega_{rz}\Delta t$) is due to shear stresses from the previous time increment, which now act as normal stresses due to the new orientation of the element caused by an incremental rotation ($\omega_{rz}\Delta t$) during the time increment. The axial stress has the same form as the radial stress, and the tangential stress is also similar except there is no contribution from rotated shear stresses.

The trial values of the shear stresses are formulated in a similar manner

$$\tau_{rz}^{t+\Delta t}=\tau_{rz}^t+G\dot{\gamma}_{rz}\Delta t+(\sigma_r^t-\sigma_z^t)\omega_{rz}\Delta t \tag{20}$$

$$\tau_{r\theta}^{t+\Delta t}=\tau_{r\theta}^t+G\dot{\gamma}_{r\theta}\Delta t \tag{21}$$

$$\tau_{z\theta}^{t+\Delta t}=\tau_{z\theta}^t+G\dot{\gamma}_{z\theta}\Delta t \tag{22}$$

The rotational terms can only be significant for stresses in the R-Z plane since the elements can rotate in this plane without experiencing strain rates. For the other stresses involving θ, the analogous rotations cannot occur without inducing strain rates, and the effect of the rotational-induced stresses is small compared to the strain rate induced stresses.

It should be recalled that Eqs. (17-22) represent trial values of the stresses and they must be reduced if they violate the Von Mises yield criterion. An equivalent stress is given by

$$\bar{\sigma}=\sqrt{(3/2)\,(s_r^2+s_z^2+s_\theta^2)+3(\tau_{rz}^2+\tau_{r\theta}^2+\tau_{z\theta}^2)} \tag{23}$$

If $\bar{\sigma}$ is not greater than the equivalent tensile strength of the material, $\bar{S}$, the final deviator and shear stresses are as given in Eqs. (17-22). If $\bar{\sigma}$ is greater than $\bar{S}$, then the stresses in Eqs. (17-22) must be multiplied by the factor ($\bar{S}/\bar{\sigma}$). When the reduced deviator and shear stresses are put into Eq. (23), the result is always $\bar{\sigma}=\bar{S}$.

The hydrostatic pressure is dependent on the volumetric strain, and sometimes the internal energy in the element. For lower impact velocities where the volumetric strain is generally small, the pressure can be adequately obtained from the bulk modulus and the volumetric strain. For higher impact velocities the effect of internal energy in the element can be significant and should be included, as it is in the Mie-Gruneisen equations of state.[5]

The artificial viscosity is combined with the normal stresses to damp out localized oscillations of the concentrated masses. It tends to eliminate spurious oscillations that would otherwise occur for wave propagation problems. This technique was originally proposed by Von Neumann and Richtmyer[6] and has been expanded for use in various computer codes.[7] It is expressed in terms of linear and quadratic components and is applied only when the volumetric strain rate is negative:

$$Q=C_L\rho c_s h\,|\dot{\epsilon}_v|+C_0^2\rho h^2\,(\dot{\epsilon}_v)^2 \quad \text{for } \dot{\epsilon}_v<0$$

$$Q=0 \quad \text{for } \epsilon_v\geq 0 \tag{24}$$

where c_s and ρ are the sound velocity and density of the material, h is the minimum altitude of the triangle, and C_L and C_0^2 are dimensionless coefficients.

Concentrated Forces

After the element stresses are obtained, it is necessary to determine concentrated forces to act on the concentrated mass at the nodes. This is done by obtaining the concentrated forces which are statically equivalent to the distributed stresses in the elements. The radial, axial, and tangential forces acting on node i of an element, are

$$F_r^i=-\pi\bar{r}[(z_j-z_m)\sigma_r+(r_m-r_j)\tau_{rz}]-(2/3)\pi A\sigma_\theta \tag{25}$$

$$F_z^i=-\pi\bar{r}[(r_m-r_j)\sigma_z+(z_j-z_m)\tau_{rz}] \tag{26}$$

$$F_\theta^i=-\pi\bar{r}[(\bar{r}/r_i)\,(z_j-z_m)\tau_{r\theta}+(r_m-r_j)\tau_{z\theta}] \tag{27}$$

In Eq. (27), the factor $\bar{r}/r_i$ is included in the expression involving the shear stress in the R-θ plane. This is necessary to satisfy the equilbrium condition in this plane, which is $(\partial\tau_{r\theta}/\partial r)+(2\tau_{r\theta}/r)=0$ (Ref. 8). It is clear from this condition that the shear stress cannot be a nonzero constant, but rather must vary as a function of the radius. This stress is dependent on $\dot{\gamma}_{r\theta}$ in Eq. (9) and is not necessarily constant since $\dot{\gamma}_{r\theta}$ involves averages of the three nodal displacements and radii. Therefore, $\bar{r}/r_i$ in Eq. (27) represents the effect of a variable shear stress in the element. The net forces at node i ($\bar{F}_r^i$, $\bar{F}_z^i$, $\bar{F}_\theta^i$) are the sum of the forces from each of the individual element forces at that node.

Equations of Motion

The equations of motion are integrated by assuming a constant velocity for each time increment. The acceleration of node i in the radial direction at time $=t$ is

$$\ddot{u}_i^t=(\bar{F}_r^i/\bar{M}_i)+r_i^t(\dot{\theta}_i^{t-})^2 \tag{28}$$

The first term is due to stress-induced forces and the second term is due to spin. The updated velocity for the next time increment is

$$\dot{u}_i^{t+}=(\dot{u}_i^{t-}+\ddot{u}_i^t\overline{\Delta t})\,(1-C_D\overline{\Delta t}/r_i^t) \tag{29}$$

where $\dot{u}_i^{t-}$ is the constant velocity for the previous time increment and $\overline{\Delta t}$ is the average of the two integration time increments about time $=t$. The expression in the second set of parentheses can be used to damp out the radial velocities to give steady-state solutions for spinning bodies. If the constant C_D is set equal to twice the sound velocity of the material, the system will be approximately critically damped and the steady-state solution will be attained rapidly. This will later be demonstrated in an example. Finally, the new radial displacement at time $=t+\Delta t$ is

$$u_i^{t+\Delta t}=u_i^t+\dot{u}_i^{t+}\Delta t \tag{30}$$

The equations of motion for the axial direction have a similar form except that the spin effects for the acceleration and the damping effects for the velocity are not included.

For angular (tangential) equations of motion it is necessary to consider the angular momentum H of each concentrated mass. This gives

$$H_i^{t+}=H_i^{t-}+r_i^t\bar{F}_\theta^i\overline{\Delta t} \tag{31}$$

By substituting $H_i=\dot{\theta}_i r_i^2\bar{M}_i$ into Eq. (31) it is possible to determine the updated rotational velocity.

$$\dot{\theta}_i^{t+}=\dot{\theta}_i^{t-}\left(\frac{r_i^t}{r_i^{t+\Delta t}}\right)^2+\frac{r_i^t\overline{\Delta t}}{(r_i^{t+\Delta t})^2}\left(\frac{\bar{F}_\theta^i}{\bar{M}_i}\right) \tag{32}$$

It should be noted that even if the net tangential force $\bar{F}_\theta^i$ is equal to zero, it is possible for the spin to change if the radius changes between times t and $t+\Delta t$. It is therefore necessary to obtain the new radial position at $t+\Delta t$ before obtaining the new rotation velocity at $t+\Delta t$.

The integration time increment must be controlled to prevent numerical instability. This is done by limiting the time

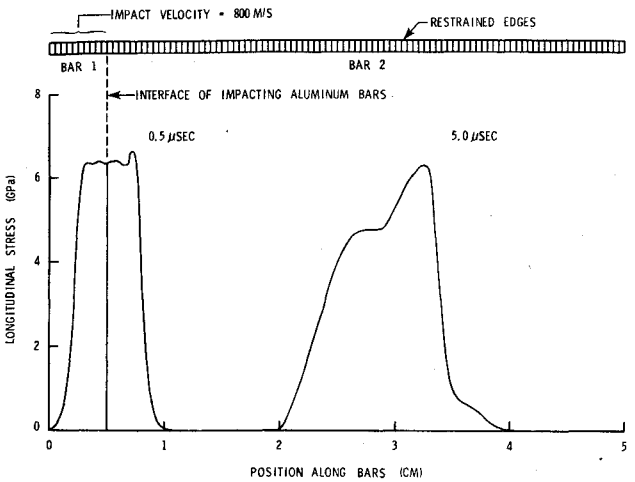

Fig. 3 Wave propagation resulting from the impact of two aluminum bars at 800 m/s.

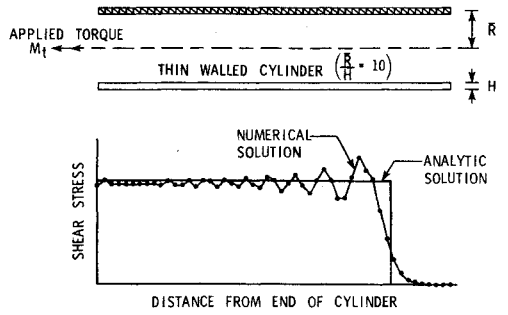

Fig. 4 Shear wave propagation in an elastic hollow cylinder.

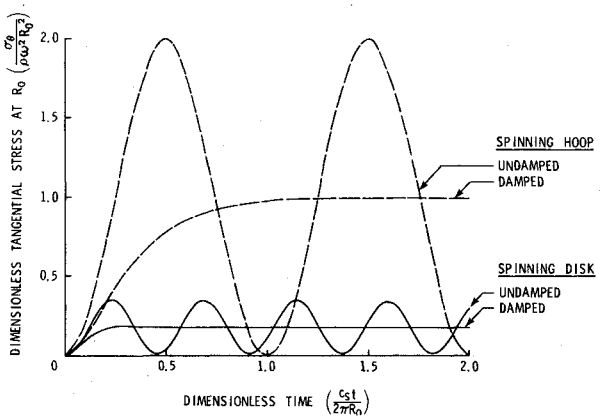

Fig. 5 Dynamic response of an elastic spinning hoop and a spinning disk subjected to a suddenly applied spin.

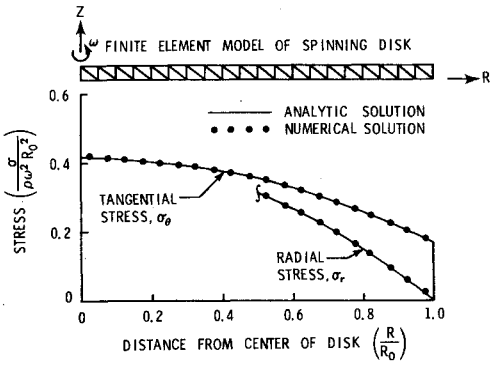

Fig. 6 Stress distribution in an elastic spinning disk.

increment to

$$\Delta t = C_t[h/(\sqrt{g^2}+\sqrt{g^2+c_s^2})] \tag{33}$$

where $g^2 = C_0^2 Q/\rho$, h is the minimum altitude of the triangle, and c_s is the second velocity.[7] The constant C_t must be less than unity to insure that Δt is always less than the time required to travel across the shortest dimension of the triangle at the sound velocity of the material.

Examples

The preceding formulation has been used to develop a computer program, EPIC-2 (Elastic-Plastic Impact Computations in 2 dimensions plus spin), and solutions to the example problems were obtained with this program. The first example, in Fig. 3, shows two aluminum bars impacting at 800 m/s. This one-dimensional problem demonstrates the capability of providing compressive wave propagation solutions. It also shows the effect of material strength with a higher-velocity elastic wave at the leading edge of the shock front and the elastic unloading at the rear. This solution is in good general agreement with that presented in Ref. 2. Additional examples of two-dimensional wave propagation in a liquid are given in Ref. 9.

The capability of providing shear wave propagation solutions is shown in Fig. 4, where a one-dimensional torque is suddenly applied to the end of a thin-walled cylinder. It can be seen that there is good general agreement between the two solutions, although the numerical solution does oscillate about the analytic solution. These oscillations exist because there is no artificial viscosity for the shear mode of deformation. The previously defined artificial viscosity in Eq. (24) is affected only by volumetric strain rates. The need for artificial viscosity in the shear mode is not as critical as for the compressive mode, however. This is because the magnitude of the shear stress is bounded by the strength of the material, whereas there is no upper bound for the magnitude of compressive waves. An example in Ref. 9 shows a compressive wave propagation solution with and without artificial viscosity. With the unbounded compressive stress, it can be seen that very radical oscillations can occur if the artificial viscosity is omitted. Since these radical oscillations cannot occur in the shear mode, due to the limitation on the strength of the material, the accuracy of the shear wave propagation solution in Fig. 4 is probably adequate for most applications.

A characteristic of spinning bodies is that transient dynamic responses are introduced if the spin is suddenly applied. This can be illustrated by considering the case of a hoop subjected to a suddenly applied spin. It can be shown that the radial stiffness of a hoop is $K = 2\pi AE/R_0$ and the mass is $M = 2\pi R_0 A\rho$, where A is the cross-sectional area, E is the modulus of elasticity R_0 is the radius, and ρ is the density. The period of vibration then becomes $T = 2\pi\sqrt{M/K} = 2\pi R_0/c_s$ where $c_s = \sqrt{E/\rho}$ is the sound velocity. Figure 5 shows the response of a hoop subjected to a suddenly applied spin ω. For this problem the hoop is represented by three nodes and one triangular element. It can be seen that the undamped spinning hoop behaves like a single-degree-of-freedom oscillator subjected to a suddenly applied force. The response is plotted as dimensionless stress as a function of dimensionless time. For the case of the spinning hoop the dimensionless stress is the ratio of the dynamic stress to the steady-state stress. Likewise, the dimensionless time is the ratio of elapsed time to the period of vibration of the spinning hoop. Both the magnitude of the response and the period of vibration are identical to those of a single-degree-of-freedom oscillator.

It is often desirable to obtain a steady-state spinning solution prior to impact. This can be done by assuming the system is critically damped until a steady-state condition is achieved. Referring again to a single-degree-of-freedom

Table 1 Summary of cylinder impact data

	Impact velocity, m/s	Initial spin ω^o rad/s	Final length, L^o	Final diameter, D^o	Maximum twist, rad	Final spin, ω^o
Test	252	0	0.842	—	0	0
HEMP	252	0	0.842	—	0	0
EPIC-2	252	0	0.853	1.49	0	0
EPIC-2	252	24,100	0.848	1.50	0.114	0.78
Test	402	0	0.635	—	0	0
HEMP	402	0	0.667	—	0	0
EPIC-2	402	0	0.684	2.15	0	0
EPIC-2	402	38,400	0.675	2.17	0.448	0.47

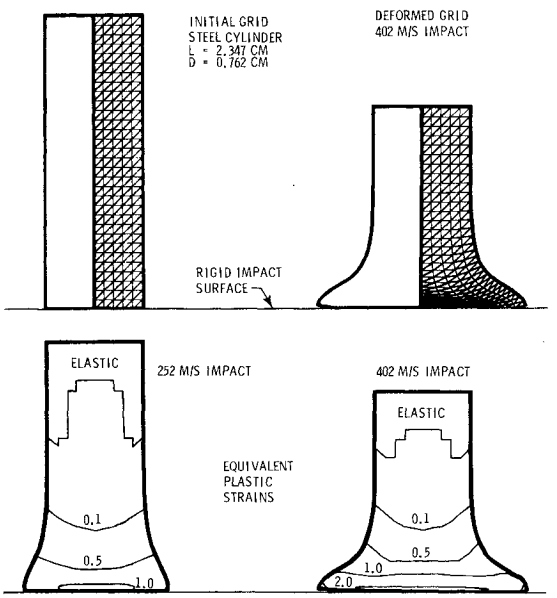

Fig. 7 Impact of a steel cylinder onto a rigid surface at 252 and 402 m/s.

system, the critical damping coefficient is $C_{crit} = 2Mc_s/R_0$. Since the resulting radial force is $F_{crit} = -C_{crit}\dot{u}$, the resulting velocity change during a time increment is $\Delta\dot{u} = F_{crit}\Delta t/M = -2c_s\Delta t\dot{u}/R_0$. This provides the basis for the damping effect in Eq. (29), where the constant C_D can be set equal to twice the sound velocity ($2c_s$).

The response of a spinning disk is also shown in Fig. 5. The basic response is similar to that of the hoop, except both the period of vibration and the magnitude of the stress are much smaller. The state of stress throughout the disk is shown in Fig. 6, and it can be seen that there is excellent agreement between the two solutions. Although the primary function of the numerical procedure is to obtain solutions for impact problems, it also provides a very efficient means of computing linear and nonlinear steady-state solutions for spinning axisymmetric solids.

The next example demonstrates the capability to represent plastic flow both with and without spin. Figure 7 shows the results of a steel cylinder striking a rigid frictionless surface at impact velocities of 252 m/s and 402 m/s. Spin is not included for the examples in this figure since the final lengths could be compared to comparable test data and HEMP simulations in Ref. 10. A summary of test data and numerical HEMP and EPIC-2 results is shown in Table 1. The numerical results use a dynamic yield strength of 1.20 GPa (Ref. 10) and they are presented for the two impact velocities. The EPIC-2 results are given for examples with and without spin. The angular velocities for the spinning examples were selected to be those which result from a rifled gun barrel with a 0.35 rad twist.

It can be seen from Table 1 that there is good agreement between the test, HEMP, and EPIC-2 results for the nonspinning impact examples. The lower portion of Fig. 7 shows equivalent plastic strain fields for the cylinders with no spin. As expected, the strains are more severe for the higher velocity impact.

For the spinning cylinders subjected to the same impact conditions, the resulting cross-sectional shapes are very similar to the nonspinning examples shown in Fig. 7. As shown in Table 1, the final deformed lengths are slightly shorter and the diameters are slightly larger. Since the addition of spin only increases the initial kinetic energy by 6.6%, no significant changes would be expected. The most interesting feature of the spinning examples is that twisting occurs along the lengths of the cylinders. This is due to the expanding diameters near the impact interface which tend to reduce the angular velocities to conserve angular momenta. The maximum twists for the two cases are 0.114 and 0.448 rad, and the final angular velocities are significantly decreased for both cases. The resulting equivalent plastic strains are slightly higher than those shown in Fig. 7.

Summary

A numerical method has been presented for axisymmetric solids subjected to impact and spin. Various example solutions have been obtained with the EPIC-2 code to demonstrate compressive and shear wave propagation, steady-state spin, and plastic flow. The addition of spin for the plastic flow impact problems introduced twisting along the length of the cylinder, but the cross-sectional geometry was not significantly affected.

Acknowledgment

This work was partially funded by Contract DAAD05-77-C-0730 from the Ballistics Research Laboratories.

References

[1] Johnson, G. R., "Analysis of Elastic-Plastic Impact Involving Severe Distortions," *Journal of Applied Mechanics*, ASME, Sept. 1976, pp. 439-444.

[2] Wilkins, M. L., "Calculations of Elastic-Plastic Flow," *Methods in Computational Physics*, Vol. 3, edited by B. Alder, S. Fernbach, and M. Rotenberg, Academic Press, New York, N.Y., 1964, pp. 211-263.

[3] Bertholf, L. D. and Benzley, S. E., "TOODY II, A Computer Program for Two-Dimensional Wave Propagation," SC-RR-68-41, Sandia Laboratories, Alburquerque, N. M., Nov. 1968.

[4] Hageman, L. J. and Walsh, J. M., "HELP, A Multi-Material Eulerian Program for Compressible Fluid and Elastic-Plastic Flows in Two Space Dimensions and Time," Vol. 1, BRL CR 39, Systems, Science and Software, LaJolla, Calif., May 1971.

[5] Walsh, J. M., et al., "Shock-Wave Compressions of Twenty-Seven Metals. Equations of State of Metals," *Physical Review*, Vol. 108, Oct. 1957, pp. 196-216.

[6] Von Neumann, J. and Richtmyer, R. D., "A Method for the Numerical Calculation of Hydrodynamic Shocks," *Journal of Applied Physics 21*, 1950, pp. 232-237.

[7] Walsh, R. T., "Finite Difference Methods," *Dynamic Response of Materials to Intense Impulsive Loading*, edited by P. C. Chou and A. K. Hopkins, Air Force Materials Laboratory, 1972, pp. 363-403.

[8] Wang, C. T., *Applied Elasticity*, McGraw-Hill, New York, 1953.

[9] Johnson, G. R., "Liquid-Solid Impact Calculations with Triangular Elements," *Journal of Fluids Engineering*, ASME, Sept. 1977, pp. 598-600.

[10] Wilkins, M. L., and Guinan, M. W., "Impact of Cylinders on a Rigid Boundary," *Journal of Applied Physics*, March 1973, pp. 1200-1206.